

Supplementary information

Surface chemistry and catalytic activity in H₂O₂ decomposition of pyrolytically fluoralkylated activated carbons

Gauhar Mussabek,^{#ab} Saule Baktygerey,^{ab} Yerzhan Taurbayev,^a Dana Yermukhamed,^{ab} Nazym Zhylkybayeva,^{ab} Alexander N. Zaderko,^c Vitaliy E. Diyuk,^{#d} Sergii Afonin,^e Gulmira Yarmukhamedova,^a Ruslan T. Mariychuk,^f Liudmyla M. Grishchenko,^d Mária Kaňuchová^g and Vladyslav V. Lisnyak^{*adhi}

-
- a.* Nanotechnological Laboratory of Open Type, Al-Farabi Kazakh National University, 050040 Almaty, Kazakhstan.
- b.* Institute of Information and Computational Technologies, 050012 Almaty, Kazakhstan.
- c.* Light Matter Institute, UMR-5306, Claude Bernard University of Lyon/CNRS, Université de Lyon, 69622 Villeurbanne Cedex, France.
- d.* Chemical Faculty, Taras Shevchenko National University of Kyiv, 01033 Kyiv, Ukraine.
E-mail: lisnyak@univ.kiev.ua
- e.* Institute of Biological Interfaces (IBG-2), Karlsruhe Institute of Technology, POB 3640, 76021 Karlsruhe, Germany.
- f.* Department of Ecology, Faculty of Humanities and Natural Sciences, University of Prešov in Prešov, 08001 Prešov, Slovakia.
- g.* Institute of Earth Resources, Faculty of Mining, Ecology, Process Control and Geotechnology, Technical University of Košice, 042 00 Košice, Slovakia.
- h.* Western Caspian University, 31, Istiglaliyyat Str., Baku AZ 1001, Republic of Azerbaijan.
- i.* Institute of Macromolecular Chemistry, the National Academy of Sciences of Ukraine, 48 Kharkivske Shose, 02160 Kyiv, Ukraine.

(19 pages, 8 figures, 7 tables, and 1 supplementary text)

	Page
Table of contents	
Fig. S1. Representative PXRD patterns.	S3
Table S1. Centers of diffraction features and interlayer distance estimated from PXRD data.	S4
Fig. S2. Representative XP core level spectra of C 1s.	S5
Table S2. Binding energy (eV) and content (%) for the C 1s components of the corresponding core levels in the XP spectra of the samples of the AC-F4 and AC-F5 series.	S6
Fig. S3. Representative XP core level spectra of O 1s.	S7
Table S3. Binding energy (eV) and content (%) for the O1s components of the corresponding core levels in the XP spectra of the samples of the AC-F4 and AC-F5 series.	S8
Table S4. Binding energy (eV) and content (%) for the F 1s components of the corresponding core levels in the XP spectra of the samples of the AC-F4 and AC-F5 series.	S9
TEXT S1	S10
Fig. S4. Comparison of two kinetic models (a) "0" and (b) "1" in fitting data points collected during volumetric measurements.	S12
Fig. S5. Effective constants obtained from treatment of experimental data: (a–c) by using the model "0" and (d–f) by using the model "1".	S13
Fig. S6. Representative conversion versus time plots for H ₂ O ₂ decomposition in water at different pH for (a) AC-F4-500 and (b) AC-F5-600 samples.	S14
Table S5. Kinetic parameters of H ₂ O ₂ decomposition in water over carbon-based catalysts at different pH levels.	S15
Fig. S7. Representative conversion versus time plots for H ₂ O ₂ decomposition in water measured at different temperatures for (a) AC-F4-500 and (b) AC-F5-600 samples.	S16
Table S6. Kinetic parameters of H ₂ O ₂ decomposition in water over carbon-based catalysts at different temperatures.	S17
Table S7. Quantitative analysis for fluorine and oxygen.	S18
Fig. S8. Correlation dependences between α_{70} and Δm_3 in the reaction of H ₂ O ₂ decomposition in water (a) and methanol (b) over prepared carbon-based catalysts.	S19

Supplementary information, Fig. S1

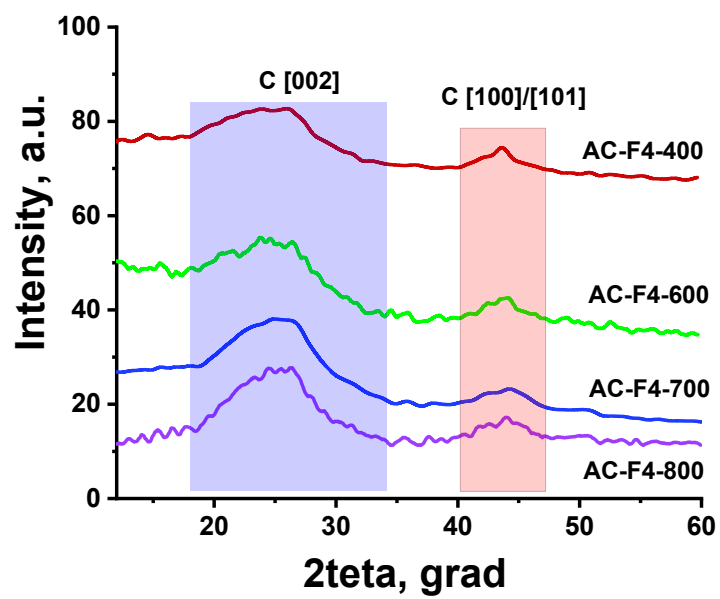


Fig. S1 Representative PXRD patterns.

Supplementary information, Table S1

Table S1 Centers of diffraction features and interlayer distance estimated from PXRD data.

Sample	2 θ , grad		Interlayer distance (nm)		Sample	2 θ , grad		Interlayer distance (nm)	
	C ₀₀₂	C ₁₀₀	d ₀₀₂	d ₁₀₀		C ₀₀₂	C ₁₀₀	d ₀₀₂	d ₁₀₀
AC-F4-800	24.56	44.32	0.362	0.204	AC-F5-800	24.25	44.22	0.367	0.204
AC-F4-700	24.54	44.28	0.363	0.204	AC-F5-700	24.75	44.15	0.359	0.205
AC-F4-600	24.26	43.71	0.367	0.207	AC-F5-600	24.10	43.65	0.369	0.207
AC-F4-400	24.11	43.57	0.369	0.208	AC-F5-400	23.85	43.05	0.373	0.210

Supplementary information, Fig. S2

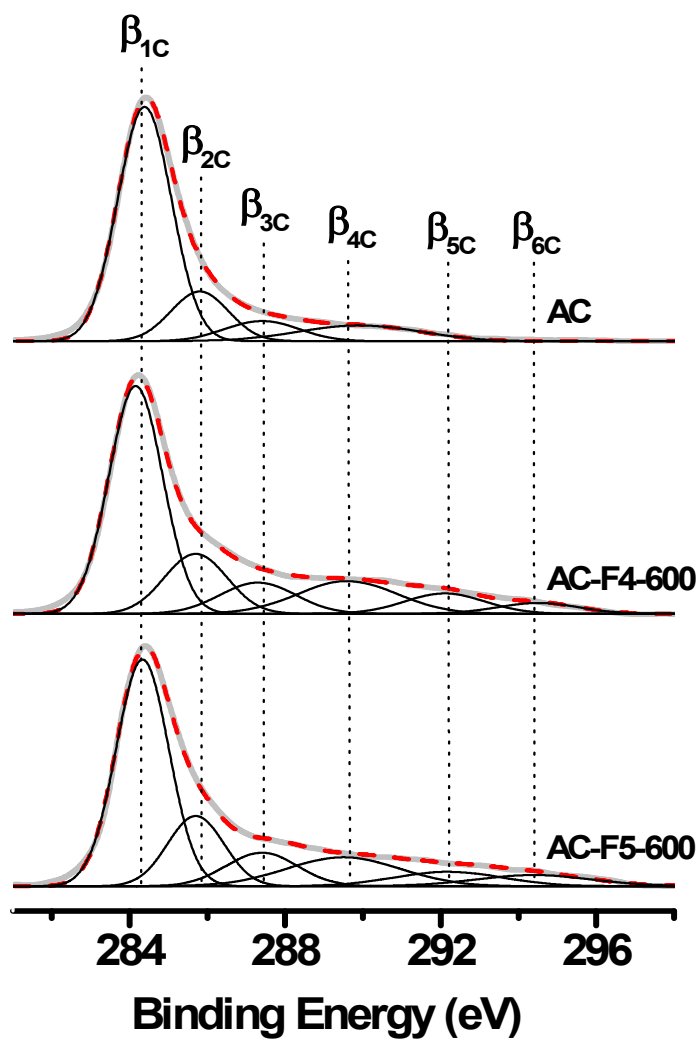


Fig. S2 Representative XP core level spectra of C 1s.

Supplementary information, Table S2

Table S2. Binding energy (eV) and content (%) for the C 1s components of the corresponding core levels in the XP spectra of the samples of the AC-F4 and AC-F5 series.

Sample	θ_{1C}	θ_{2C}	θ_{3C}	θ_{4C}	θ_{5C}	θ_{6C}
	C=C	C–O	C=O, C–F	O–C=O, CF–(CF _x)	CF ₂	CF ₃
AC	284.3 (66.9)	285.8 (15.1)	287.4 (7.7)	289.9 (10.3)	–	–
AC-F4-600	284.2 (51.1)	285.7 (15.5)	287.3 (9.7)	289.6 (13.4)	292.1 (6.7)	294.5 (3.6)
AC-F4-700	284.3 (52.4)	285.7 (15.8)	287.4 (10.1)	289.6 (12.8)	292.0 (6.4)	294.6 (2.5)
AC-F4-800	284.3 (53.2)	285.7 (16.4)	287.3 (10.5)	289.6 (12.4)	292.1 (5.5)	294.6 (2.0)
AC-F5-600	284.3 (48.7)	285.7 (16.0)	287.4 (9.8)	289.5 (16.6)	292.2 (6.4)	294.4 (5.5)
AC-F5-700	284.3 (49.6)	285.9 (16.8)	287.5 (10.2)	289.8 (15.3)	291.9 (4.3)	293.8 (3.8)
AC-F5-800	284.4 (51.7)	285.7 (17.2)	287.4 (10.6)	289.9 (14.4)	291.9 (3.3)	293.4 (2.8)

Supplementary information, Fig. S3

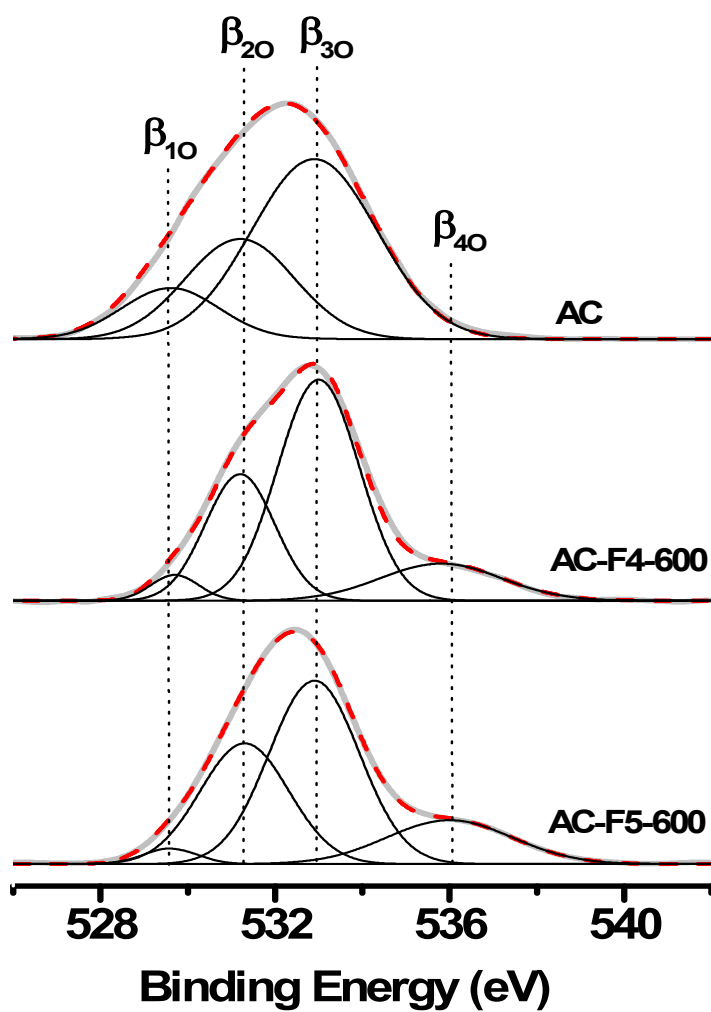


Fig. S3 Representative XP core level spectra of O 1s.

Supplementary information, Table S3

Table S3. Binding energy (eV) and content (%) for the O1s components of the corresponding core levels in the XP spectra of the samples of the AC-F4 and AC-F5 series.

Sample	θ_{10}	θ_{20}	θ_{30}	θ_{40}
	O–C=O	C=O	C–O	C–O (F)
AC	529.6 (13.0)	531.2 (28.3)	532.9 (58.7)	–
AC-F4-600	529.7 (3.8)	531.2 (27.1)	533.0 (55.2)	535.9 (13.9)
AC-F4-700	529.7 (3.1)	531.4 (37.9)	533.0 (46.7)	535.9 (12.3)
AC-F4-800	529.7 (2.6)	531.4 (50.4)	533.1 (41.2)	535.9 (5.8)
AC-F5-600	529.6 (2.4)	531.3 (31.7)	533.0 (48.8)	536.0 (17.1)
AC-F5-700	529.7 (2.0)	531.4 (38.6)	533.0 (44.4)	535.9 (15.0)
AC-F5-800	529.7 (1.9)	531.4 (52.9)	533.1 (38.3)	535.9 (6.9)

Supplementary information, Table S4

Table S4. Binding energy (eV) and content (%) for the F 1s components of the corresponding core levels in the XP spectra of the samples of the AC-F4 and AC-F5 series.

Sample	θ_{1F}	θ_{2F}	θ_{3F}	θ_{4F}
	C-F _{SI}	C-F	CF ₂	CF ₃
AC-F4-600	685.4 (10.1)	687.2 (58.9)	688.6 (18.1)	690.9 (12.9)
AC-F4-700	685.5 (18.1)	687.2 (57.5)	688.4 (14.3)	690.8 (10.1)
AC-F4-800	685.4 (29.5)	687.1 (54.9)	688.5 (8.9)	690.7 (6.7)
AC-F5-600	685.5 (13.1)	687.1 (52.3)	688.5 (18.8)	690.8 (15.9)
AC-F5-700	685.5 (19.7)	687.2 (53.3)	688.5 (15.6)	690.8 (11.4)
AC-F5-800	685.5 (27.6)	687.1 (54.6)	688.5 (10.6)	690.7 (7.2)

Supplementary information, TEXT S1

The rate of the decomposition reaction in which AC catalyzes the conversion of H_2O_2 can be represented as follows:

$$r = -\frac{dC_{H_2O_2}}{d\tau} = \frac{k_2 K_M^{-1} C_C^* C_{H_2O_2}}{1 + K_M^{-1} C_{H_2O_2}}, \quad (S1)$$

where $C_{H_2O_2}$ is the concentration of H_2O_2 , C_C^* is the concentration of catalysts, k_2 is the reaction rate of the second step (see the scheme in Fig. 12), and K_M is the Michaelis constant.

From the denominator of Eq. (S1), if the catalyst forms a stable complex with a reagent, e.g., the catalyst in the reaction medium is mostly bound to a complex with a reagent, the following can be assumed:

$$K_M^{-1} C_{H_2O_2} \gg 1, \quad (S2)$$

when Eqn. (S3) becomes the zeroth-order equation with respect to H_2O_2 , hereinafter referred to as the "0" model,

$$r = -\frac{dC_{H_2O_2}}{d\tau} = k_2 C_C^*, \quad (S3)$$

When the affinity between the catalyst and the reagent is low

$$K_M^{-1} C_{H_2O_2} \ll 1 \quad (S4)$$

and Eqn. (S3) becomes the first-order equation with respect to H_2O_2 , hereinafter referred to as the "1" model,

$$r = -\frac{dC_{H_2O_2}}{d\tau} = k_2 K_M^{-1} C_C^* C_{H_2O_2} \quad (S5)$$

For processes without catalyst decontamination, the initial concentration of the added catalyst is constant, $C_C^* = C_0$. When the active sites are irreversibly deactivated, this value can be represented as the sum of the concentrations of the more active initial (C_i) and less active final (C_f) states of a catalyst.

The process of irreversible deactivation of the active sites is a first-order reaction with respect to the catalyst, resulting in a decrease in the activity of the AC with respect to the peroxide decomposition:



where k_d is the decay constant.

Taking into account the deactivation, the concentration of the initial and final states of the active sites of the catalyst is given by the equations:

$$C_i = C_0 e^{-k_d \tau} \quad (\text{S7})$$

$$C_f = C_0 (1 - e^{-k_d \tau}) \quad (\text{S8})$$

Taking into account Eqns. (S7) and (S8), Eqns. (S3) and (S5) can be written as

$$r = -\frac{dC_{\text{H}_2\text{O}_2}}{d\tau} = k_2 C_0 e^{-k_d \tau} + k_2' C_0 (1 - e^{-k_d \tau}) = k_{0i} e^{-k_d \tau} + k_{0f} (1 - e^{-k_d \tau}) \quad (\text{S9})$$

$$r = -\frac{dC_{\text{H}_2\text{O}_2}}{d\tau} = k_2 K_M^{-1} C_0 C_{\text{H}_2\text{O}_2} e^{-k_d \tau} + k_2' K_M^{-1} C_0 C_{\text{H}_2\text{O}_2} (1 - e^{-k_d \tau}) = k_{1i} C_{\text{H}_2\text{O}_2} e^{-k_d \tau} + k_{1f} C_{\text{H}_2\text{O}_2} (1 - e^{-k_d \tau}) \quad (\text{S10})$$

where k_{0i} , k_{0f} , k_{1i} , and k_{1f} are effective constants. These constants, considered in pairs, k_{0i} and k_{1i} and k_{0f} and k_{1f} characterize the initial and final activity of a catalyst in the H_2O_2 decomposition reaction, respectively. The decay constant k_d characterizes the rate of transition from the initial to the final state of active catalyst sites.

Eqns. (9) and (10) are mathematical models describing the decomposition of H_2O_2 with the participation of two states of the active sites. Their integral forms, followed by the models "0" and "1", in terms of the reaction order with respect to hydrogen peroxide, are defined as

$$C_{\text{H}_2\text{O}_2} = C_{\text{H}_2\text{O}_2}^0 - k_{0f} \tau - \frac{k_{0i} - k_{0f}}{k_d} + \frac{k_{0i} - k_{0f}}{k_d} e^{-k_d \tau} \quad (\text{S11})$$

$$\ln C_{\text{H}_2\text{O}_2} = \ln C_{\text{H}_2\text{O}_2}^0 - k_{1f} \tau - \frac{k_{1i} - k_{1f}}{k_d} + \frac{k_{1i} - k_{1f}}{k_d} e^{-k_d \tau} \quad (\text{S12})$$

Eqns. (S11) and (S12) were used to fit the experimental data by a nonlinear least squares method in Origin software (Origin Lab, Northampton, MA, USA). The parameter characterizing the fit of the mathematical models to the experimental data was the χ^2 -factor, which was assigned to the total number of points on the curve (100 points). Fig. S4 shows typical kinetic curves that were fitted with the proposed mathematical models.

Apparently, both models well describe the experimental data. For the whole dataset, the proposed models give similar results; model "1" is slightly more precise, as evidenced by somewhat lower values of χ^2/n (see Table 8).

Supplementary information, Fig. S4

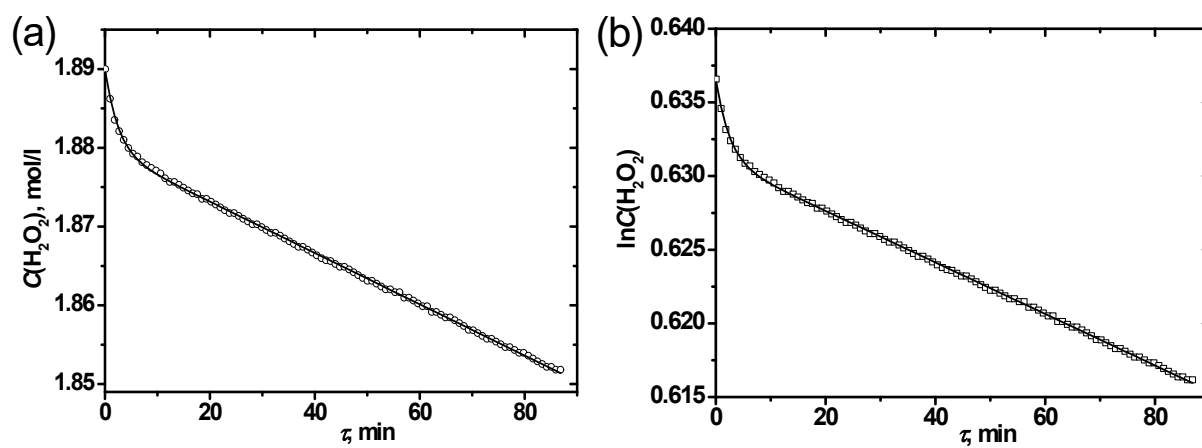


Fig. S4 Comparison of two kinetic models (a) "0" and (b) "1" in fitting data points collected during volumetric measurements.

Supplementary information, Fig. S5

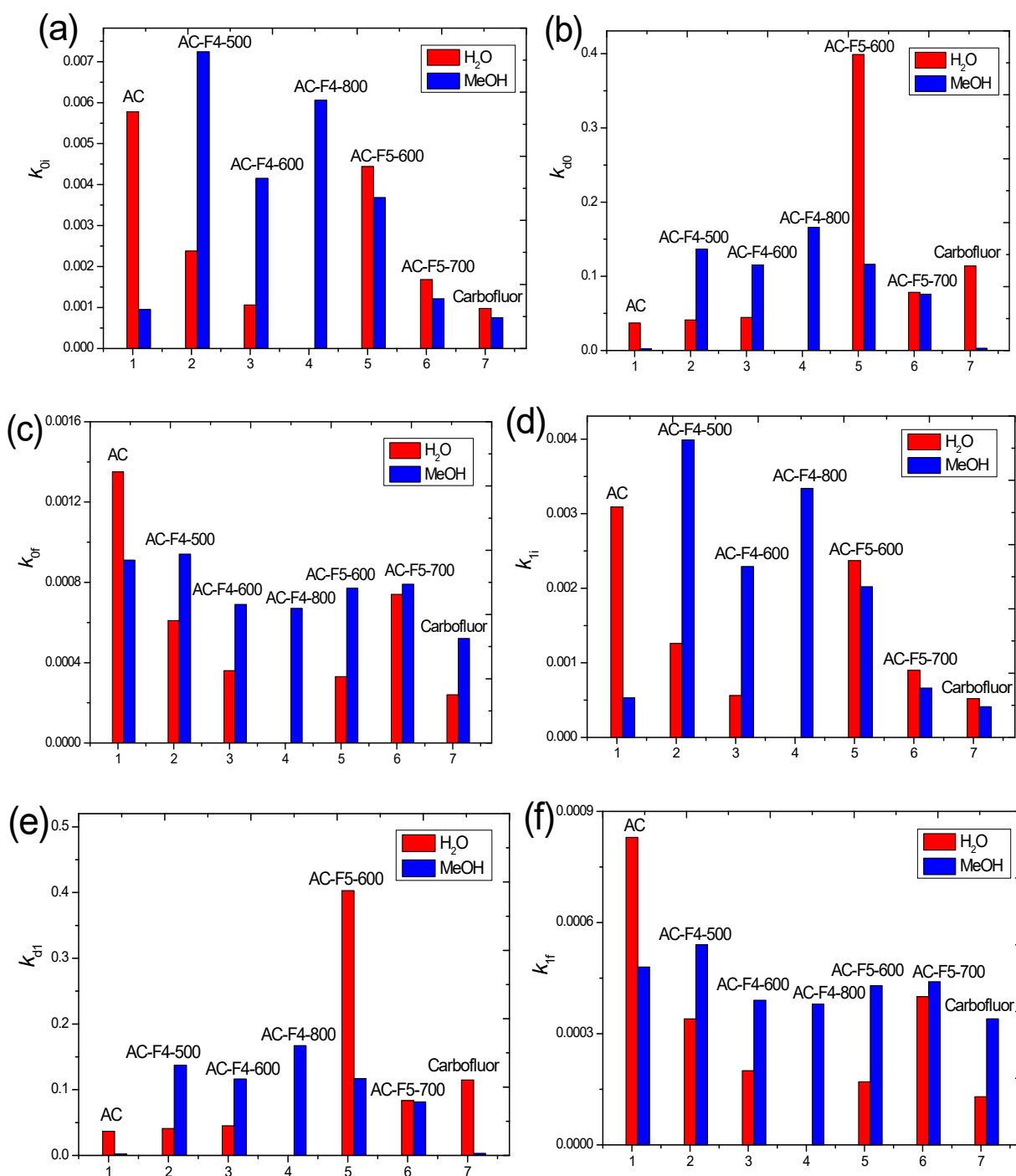


Fig. S5 Effective constants obtained from treatment of experimental data: (a-c) by using the model "0" and (d-f) by using the model "1".

Supplementary information, Fig. S6

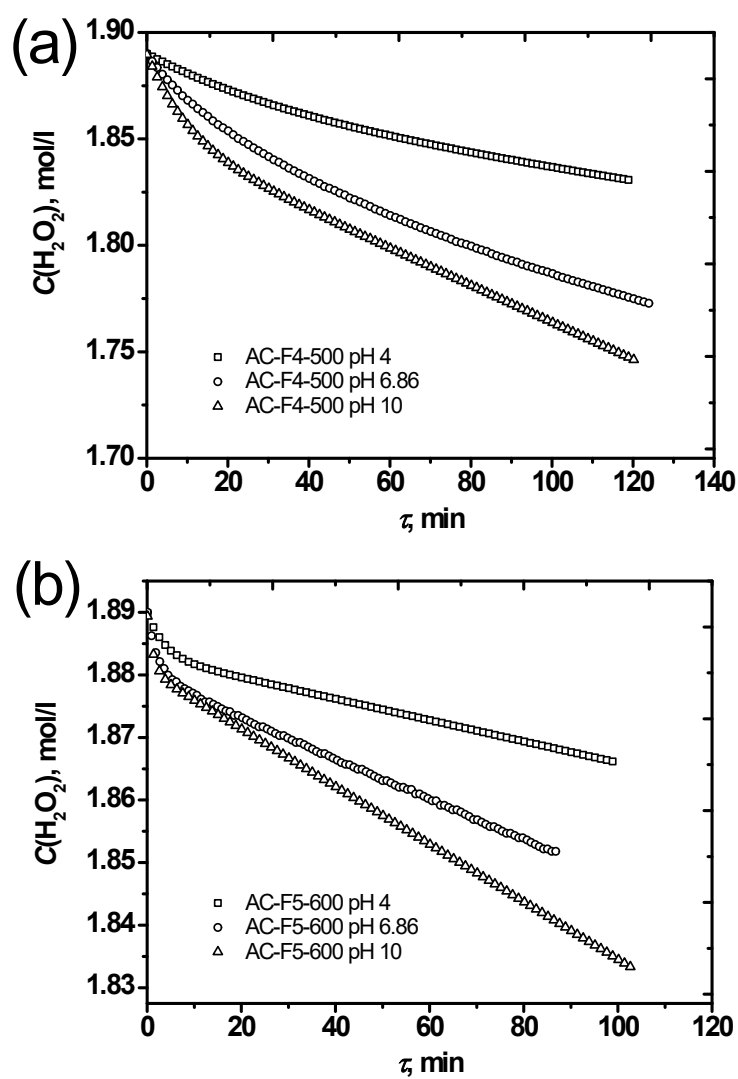


Fig. S6. Representative conversion versus time plots for H_2O_2 decomposition in water at different pH for (a) AC-F4-500 and (b) AC-F5-600 samples.

Supplementary information, Table S5

Table S5 Kinetic parameters of H₂O₂ decomposition in water over carbon-based catalysts at different pH levels.

pH	α_{70} (%)	$k_{0i} \times 10^3$ (mol \times min ⁻¹)	$k_d \times 10^2$ (min ⁻¹)	$k_{0f} \times 10^4$ (mol \times min ⁻¹)	$^a(\chi^2/n)$ $\times 10^{-6}$	$k_{1i} \times 10^3$ (min ⁻¹)	$k_d \times 10^2$ (min ⁻¹)	$k_{1f} \times 10^4$ (min ⁻¹)	$^a(\chi^2/n)$ $\times 10^{-7}$
Sample AC-F4-500									
4	2.28	1.01	2.71	2.8	0.20	0.54	2.73	1.5	0.42
6.86	4.42	2.38	4.10	6.1	0.24	1.26	4.10	3.4	0.65
10	5.30	4.71	9.78	8.7	0.19	2.53	10.13	4.8	0.31
Sample AC-F5-600									
4	1.01	2.02	27.26	1.7	0.15	1.11	27.45	0.9	0.24
6.86	1.76	4.44	39.89	3.3	0.03	2.37	40.28	1.7	0.08
10	2.22	7.85	78.24	4.7	0.21	4.24	80.72	2.5	0.11

Supplementary information, Fig. S7

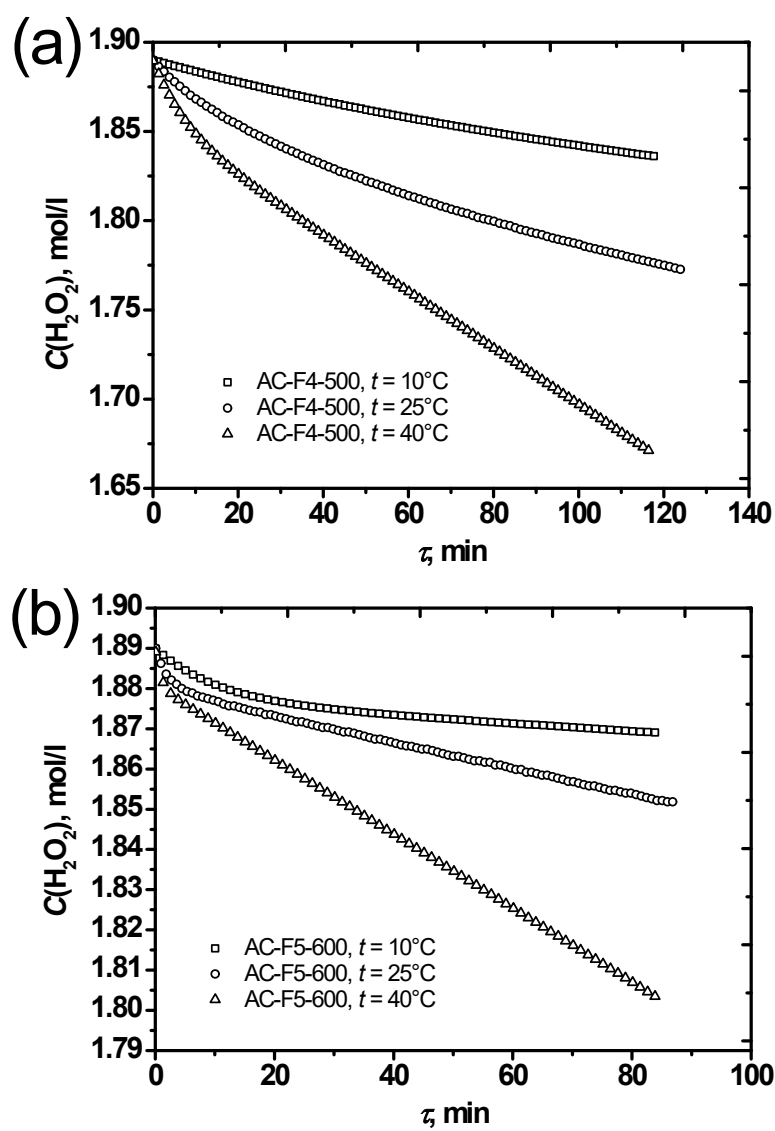


Fig. S7. Representative conversion versus time plots for H_2O_2 decomposition in water measured at different temperatures for (a) AC-F4-500 and (b) AC-F5-600 samples.

Supplementary information, Table S6

Table S6 Kinetic parameters of H₂O₂ decomposition in water over carbon-based catalysts at different temperatures.

<i>t</i> , °C	α_{70} (%)	$k_{0i} \times 10^3$ (mol \times min ⁻¹)	$k_d \times 10^2$ (min ⁻¹)	$k_{0f} \times 10^4$ (mol \times min ⁻¹)	$a(\chi^2/n)$ $\times 10^{-6}$	$k_{1i} \times 10^3$ (min ⁻¹)	$k_d \times 10^2$ (min ⁻¹)	$k_{1f} \times 10^4$ (min ⁻¹)	$a(\chi^2/n)$ $\times 10^{-7}$
Sample AC-F4-500									
10	1.96	0.66	0.98	1.7	0.22	0.35	0.94	0.9	0.35
25	4.42	2.38	4.10	6.1	0.24	1.26	4.10	3.4	0.65
40	7.72	6.08	12.94	15.8	0.27	3.39	14.79	9.1	0.44
<i>E</i> (kJ\timesmol⁻¹)	–	55 \pm 3	60 \pm 4	56 \pm 3	–	55 \pm 3	68 \pm 1	57 \pm 3	–
Sample AC-F5-600									
10	1.06	1.35	9.61	0.9	0.19	0.72	9.58	0.5	0.24
25	1.76	4.44	39.89	3.3	0.03	2.37	40.28	1.7	0.08
40	3.92	11.53	112.8	9.2	0.21	6.87	136.6	5.1	0.34
<i>E</i> (kJ\timesmol⁻¹)	–	53 \pm 2	61 \pm 4	56 \pm 2	–	55 \pm 1	65 \pm 1	55 \pm 1	–

Supplementary information, Table S7

Table S7 Quantitative analysis for fluorine and oxygen.

Sample	C_F (mmol g ⁻¹)			C_F (EDS)/ C_F (CA)	C_F (XPS)/ C_F (CA)	C_O (mmol g ⁻¹)		C_O (XPS)/ C_O (CHNS)
	^a CA	EDS	XPS			CHNS	XPS	
^b AC-F4-400	0.11	0.33	3.95	3.0	35.9	3.28	19.0	5.8
^b AC-F4-500	0.39	0.41	4.36	1.1	11.2	3.11	17.1	5.5
AC-F4-600	1.93	3.01	7.49	1.6	3.9	2.90	7.84	2.7
AC-F4-700	1.87	2.83	5.95	1.5	3.2	2.98	7.16	2.4
AC-F4-800	1.75	2.67	4.81	1.5	2.7	3.15	6.92	2.2
^b AC-F5-400	0.09	0.17	1.82	1.9	20.2	2.41	13.4	5.6
^b AC-F5-500	0.72	0.74	6.23	1.0	8.7	2.63	13.4	5.1
AC-F5-600	2.30	3.54	8.50	1.5	3.7	3.05	7.31	2.4
AC-F5-700	2.94	2.83	5.94	0.96	2.0	3.14	6.91	2.2
AC-F5-800	1.69	2.60	4.41	1.5	2.6	3.23	7.11	2.2

^aThe chemical analysis (CA) results presented here were obtained by means of ion-selected potentiometry; ^bThe data were taken from Ref. (24).

Supplementary information, Fig. S8

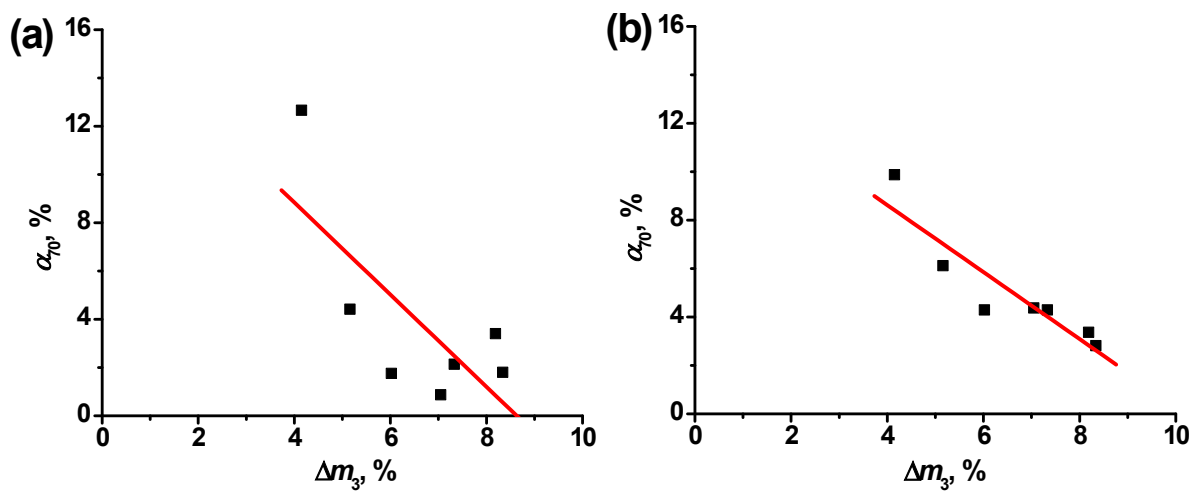


Fig. S8. Correlation dependences between α_{70} and Δm_3 in the reaction of H_2O_2 decomposition in water (a) and methanol (b) over prepared carbon-based catalysts.